Nonlinear Feedforward Control for Wind Disturbance Rejection on Autonomous Helicopter

Bisgaard, Morten; la Cour-Harbo, Anders; A. Danapalasingam, Kumeresan

Published in:
IEEE/RSJ International Conference on Intelligent Robots and Systems

DOI (link to publication from Publisher):
10.1109/IROS.2010.5651755

Publication date:
2010

Document Version
Early version, also known as pre-print

Nonlinear Feedforward Control for Wind Disturbance Rejection on Autonomous Helicopter

Morten Bisgaard, Anders la Cour-Harbo, Kumeresan A. Danapalasingam

Abstract— **This paper presents the design and verification of a model based nonlinear feedforward controller for vertical and horizontal wind disturbance rejection on autonomous helicopters. The feedforward control is based on a helicopter model that is derived using a number of carefully chosen simplifications to make it suitable for the purpose. The model is inverted for the calculation of rotor collective and cyclic pitch angles given the wind disturbance. The control strategy is then applied on a small helicopter in a controlled wind environment and the effectiveness and advantage of the feedforward controller is demonstrated through flight tests.**

I. INTRODUCTION

Autonomous helicopters are small-scale helicopters, mostly equipped with on-board intelligence capable of performing various tasks like surveillance, search and rescue, law enforcement, aerial mapping, cinematography, inspection, etc. In this paper a feedforward control scheme capable of rejecting wind disturbances on the helicopter will be developed. The concept is to measure the wind disturbance at the helicopter and countering it before it can affect the position of the helicopter.

Sudden changes in wind can occur for instance when flying in an urban environment. An example of a system where wind disturbance rejection can be crucial is an emergency vehicle assistance system, where a small helicopter fly autonomously some distance in front of, say, an ambulance. The helicopter leapfrogs between intersections along the route of the ambulance, alerting nearby traffic to stay clear and report any possible problems ahead to the ambulance driver. An application like this requires, among other things, high performance control since the helicopter will operate in close proximity to obstacles like buildings, power lines, street lights, etc. Only very little error margin can be allowed in the trajectory tracking control and therefore the design of high performance controllers that could reject known and unknown disturbances to produce desired flight quality is crucial. When flying through a road intersection, sudden cross winds can be difficult to handle, even for a high performance feedback controller.

Another example where wind disturbance rejection is important is the use of an autonomous helicopter for inspection of offshore wind turbines and oil rig flare towers. The helicopter must operate very close to the turbine or tower and can easily experience very strong wind gusts which can lead to potentially dangerous situations.

The authors are with the Department of Electronic Systems, Section for Automation and Control, Aalborg University, 9220 Aalborg East, Denmark {bisgaard,alc,kad}@es.aau.dk

This paper presents the design of a model based feedforward controller to counter wind disturbance effects on autonomous helicopters. This is achieved by deriving a simplified helicopter model in section II. This model is then used for the design of the feedforward controller in section III. In section V results are presented from flight tests of the feedforward controller in a controlled environment and finally a discussion and conclusion is given in section VI.

A. Previous Work

To date numerous feedback controller designs for autonomous helicopters have been accomplished with good results, but only little attention has been given to feedforward type control.

Nonlinear model predictive control (MPC) based on a neural network is used in conjunction with state dependent Riccati equation (SDRE) control in [1] for helicopter control. The SDRE controller provides robust stabilization of the helicopter using a simplified model while the neural MPC uses high fidelity nonlinear models for improved performance. The neural MPC was trained to include wind fields and simulations using a high fidelity wind model, including eddies and turbulence, and by accounting for the wind in a feedforward manner in the MPC, performance could be significantly improved. However, the use of nonlinear MPC – and also SDRE – as means of stabilizing the helicopter has the disadvantage that a highly intensive computational effort is needed for real time implementation of the control scheme. It can be difficult to achieve real time control of a small high-bandwidth helicopter with such methods. Therefore, a control system based only on SDRE, but with a nonlinear feedforward compensation to account for model simplifications has been proposed [2]. Good tracking performance is shown on two different helicopters. The nonlinear feedforward compensator is shown to be able to improve performance if provided with a static estimate of the wind conditions.

An adaptive trajectory tracking controller is presented in [3] where inverse dynamics together with a neural network is used for feedback linearization. The actual design is done using a cascading principle with a attitude controlling inner loop and a translational controlling outer loop. PD feedback from a reference model error is used to suppress disturbances and shape the two loops. The controller has been tested on a wide range of flying vehicles and has shown excellent tracking performance in a wide flight envelope, while being robust to changes in vehicle parameters. The approach with

dynamic inversion resembles feedforward control and could most likely be extended to account for wind disturbances.

A feedforward control strategy augmented to an existing feedback controller is demonstrated for an autonomous helicopter in [4]. The purpose of the feedforward controller is to assist the feedback loop in rejecting wind disturbances based on wind velocity measurements made onboard the helicopter. The feedforward control actions are obtained through trimming of the helicopter model subjected to a simulated wind. These different trim points in state space are then used as training input for a neural network that is then used as the online feedforward controller. Simulations, using measured wind profiles, showed the feasibility of this approach for wind disturbance rejection. Stability for a nonlinear feedforward controller for wind disturbance rejection has been proven [5]. In a similar field, results on the use of feedforward on wind turbines to react to wind changes have been reported [6].

II. HELICOPTER MODEL

The helicopter model derived here is intended for use directly in the feedforward control and is a simplified version of the AAU Helisim model [7][1]. This simplified version neglects hinge offset and servo actuator dynamics. Inflow is assumed uniform and main rotor and stabilizer bar are considered steady state. The model is derived using blade element analysis and momentum theory.

While the model derived here is similar to models found in other literature, it is chosen to describe it thoroughly here as a number of specific assumptions are take to make it feasible for inversion.

In the following the velocity of the helicopter with respect to a inertial reference frame is denoted $v = [v_x, v_y, v_z]$ and the helicopter aerodynamic velocity, i.e. including external wind, is denoted $w = [w_x, w_y, w_z]$. The blade advance ratio μ and rotor inflow ratio (λ) are defined as

$$\mu_x = \frac{w_x}{\Omega R}, \quad \mu_y = \frac{w_y}{\Omega R}, \quad \mu_z = \frac{w_z}{\Omega R}, \quad \lambda = \frac{w_z - v_i}{\Omega R}. \tag{1}$$

where v_i is the rotor induced velocity, R is blade length, Ω is rotor angular velocity, and $\mu = [\mu_x \;\; \mu_y \;\; \mu_z]^T$.

At any given azimuth station φ, the pitch of a point on a rotor blade (see figure 1) can be described by

$$\theta_r = \theta_{\text{col}} - \theta_{\text{lat}} \cos(\varphi) - \theta_{\text{lon}} \sin(\varphi) + \theta_t \frac{r}{R}, \tag{2}$$

where θ_{col} is the collective, θ_{lat} and θ_{lon} are cyclic pitch, θ_t is the blade twist, and r is the distance to the point of the blade. The flapping motion of the main rotor can be well approximated by the first terms of Fourier series

$$\beta = a_{con} - a_{\text{lon}} \cos(\varphi) + a_{\text{lat}} \sin(\varphi), \tag{3}$$

which consists of the coning angle a_{con} as well as the longitudinal a_{lon} and lateral a_{lat} flapping angles. Figure 1 shows a blade cross section with the two forces affecting the infinitesimal blade element dr: The lift dL and the drag dD. The lift and drag are defined as force perpendicular and parallel, respectively, to the blade velocity. The lift on a small

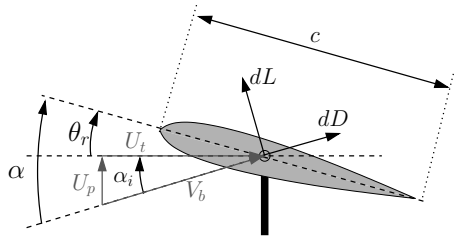

Fig. 1. Cross section of the blade showing the blade element forces.

blade element can be described as

$$dL = \frac{1}{2} \rho V_b^2 C_l \alpha c \;\; dr \tag{4}$$

with air density ρ, blade velocity V_b, size of the blade (cord length) c, blade lift curve slope C_l, and blade angle of attack α. As is shown on figure 1 the angle of attack is equal to the sum of the pitch angle θ_r and the local inflow angle α_i. This means that the angle of attack can be described by

$$\alpha = \theta_r + \alpha_i = \theta_r + \frac{U_t}{U_p}, \tag{5}$$

where α_i is approximately equal to the ratio of the horizontal (U_t) to the vertical (U_p) elements of V_b when assuming that the induced velocity is much smaller that the rotational velocity of the blade. This assumption also gives

$$V_b = \sqrt{U_t^2 + U_p^2} \simeq U_t, \tag{6}$$

which leads to the final description of the lift as

$$dL = \frac{1}{2} \rho U_t^2 C_l c \left(\theta_r + \frac{U_t}{U_p} \right) \;\; dr. \tag{7}$$

The drag dD on the blade element can be described similar to the lift

$$dD = \frac{1}{2} \rho V_b^2 C_d c \;\; dr, \tag{8}$$

where C_d is the blade drag coefficient.

Two different contributions can be identified for the horizontal blade velocity. The rotation of the blade around the shaft and the helicopter motion. The contribution from the helicopter motion can be expressed as the translational velocities mapped to the blade by the blade azimuth station and together with element from the blade rotation it forms U_t as

$$U_t \simeq \Omega R \left(\frac{r}{R} + \mu_x sin(\varphi) - \mu_y cos(\varphi) \right). \tag{9}$$

It is here assumed that the vertical blade velocity consists simply of the induced velocity from the rotor which result in

$$U_p \simeq \Omega R \big(\lambda - \mu_x \beta \cos(\varphi) - \mu_y \beta \sin(\varphi) \big) - \dot{\beta} r. \tag{10}$$

[1]The AAU Helisim model can be downloaded for Matlab/Simulink at http://www.uavlab.org

A. Flapping

The flapping of the main rotor and stabilizer bar is an integral part of the helicopter dynamics. However, both rotors have dynamics that are significantly faster than the rigid body dynamics and it is therefore in this case reasonable to consider them steady state.

In order to determine the dynamic flapping motion we use an equilibrium equation of the blade torques

$$\tau_a + \tau_{cf} + \tau_\beta = 0 \tag{11}$$

where the torques in order of appearance are aerodynamic, centrifugal, and inertial torque. Effects from helicopter motion are neglected and therefore Coriolis torque and torque from body angular and normal acceleration are zero. Furthermore, the torque due to the flexing of the blade is neglected as it is typically orders of magnitude smaller than the centrifugal torque.

The aerodynamic torque is the primary torque and it originates from the lift force acting on a blade. The torque around the flapping hinge is found by integrating the lift dL over the blade length to R and multiplying with the lever r. This yields

$$\tau_a = \int_0^R \frac{1}{2}\rho U_t^2 C_l c\left(\theta_r + \frac{U_t}{U_p}\right) r \;\; dr\,. \tag{12}$$

The centrifugal force acts perpendicular to the rotation axis and as the blade flaps this results in a torque around the flapping hinge. Assuming a small flapping angle, the centrifugal force can be found as

$$\tau_{cf} = -\Omega^2 I_b \beta\,, \tag{13}$$

where I_b is the blade moment of inertia. The torque due to flapping originates from the blade angular acceleration around the flapping hinge and can be expressed as

$$\tau_\beta = -I_b \ddot{\beta}\,. \tag{14}$$

The different torques are substituted into (11) and all higher harmonics are discarded. To find the tip-path plane dynamics, the elements containing $\sin(\varphi)$ form the equation for $\ddot{a_{\text{lat}}}$ and the elements containing $\cos(\varphi)$ form the equation for $\ddot{a_{\text{lon}}}$. Coning is neglected, effects from helicopter motion are discarded and all flapping derivatives are zeroed due to the steady state assumption. The resulting simplified equations are solved for the flapping angles and yields

$$a_{\text{lat}} = -2\left(\frac{4}{3}\theta_{\text{col}} + \theta_t + \lambda\right)\mu_y - \theta_{\text{lat}} \tag{15}$$

$$a_{\text{lon}} = \;\; 2\left(\frac{4}{3}\theta_{\text{col}} + \theta_t + \lambda\right)\mu_x - \theta_{\text{lon}} \tag{16}$$

The flapping of the stabilizer bar is mixed with the pitch input from the swashplate through the Bell-Hiller gain and works as a rate-stabilizing feedback. It can be calculated in a similar fashion to the main rotor, but for most helicopters the deciding factor for the stabilizer bar flapping is the helicopter rotation and wind has little influence on it. Therefore, while the stabilizer bar is a very important part of the helicopter dynamics, it is resonable in this case to assume

$$a_{\text{lat},st} = -\theta_{\text{lat}}, \quad a_{\text{lon},st} = \theta_{\text{lon}}\,, \tag{17}$$

which effectively means that the control rotor has no influence on the feedforward.

B. Rotor Forces

Using these assumptions the infinitesimal force equations can be simplified to

$$\begin{aligned} dF_{x_{mr}} &= -dD\sin(\varphi) + dL(\beta\cos(\varphi) \pm \alpha_i \sin(\varphi))\,,\\ dF_{y_{mr}} &= \;\; dD\cos(\varphi) + dL(\beta\sin(\varphi) - \alpha_i\cos(\varphi))\,,\\ dF_{z_{mr}} &= -dL\,. \end{aligned}$$

The infinitesimal forces are then integrated over r along the blade from 0 to $R-e$. Averaging over one revolution is done by one more integration. Finally, the resulting forces are found by multiplying with the number of blades b

$$F_x = \frac{bc}{2\pi}\frac{\rho}{2}\int_0^{2\pi}\int_0^R U_t^2\left(C_l\left(\theta_r + \frac{U_p}{U_t}\right)\frac{U_p}{U_t}\sin(\varphi) - C_d\sin(\varphi)\right)\, dr d\varphi\,, \tag{18}$$

$$F_y = \frac{bc}{2\pi}\frac{\rho}{2}\int_0^{2\pi}\int_0^R U_t^2\left(-C_l\left(\theta_r + \frac{U_p}{U_t}\right)\frac{U_p}{U_t}\cos(\varphi) + C_d\cos(\varphi)\right)\, dr d\varphi\,, \tag{19}$$

$$F_z = -\frac{bc}{2\pi}\frac{\rho}{2}C_l\int_0^{2\pi}\int_0^R U_t^2\left(\theta_r + \frac{U_t}{U_p}\right)\;\; dr d\varphi\,. \tag{20}$$

Solving the integrals yields

$$F_x = \frac{1}{2}\rho C_l bc\Omega^2 R^3\left(\left(\frac{1}{2}\mu_x\lambda - \frac{1}{3}a_{\text{lon}}\right)\theta_{\text{col}} - \frac{3}{4}\lambda a_{\text{lon}} + \frac{1}{4}\left(\mu_x\lambda - a_{\text{lon}}\right)\theta_t + \frac{1}{4}\left(\mu_x a_{\text{lon}} - \lambda\right)\theta_{\text{lon}} - \frac{Cd\mu_x}{2a}\right), \tag{21}$$

$$F_y = \frac{1}{2}\rho C_l bc\Omega^2 R^3\left(\left(\frac{1}{2}\mu_y\lambda + \frac{1}{3}a_{\text{lat}}\right)\theta_{\text{col}} + \frac{3}{4}\lambda a_{\text{lat}} + \frac{1}{4}\left(\mu_y\lambda + a_{\text{lon}}\right)\theta_t + \frac{1}{4}\left(\mu_y a_{\text{lat}} + \lambda\right)\theta_{\text{lat}} - \frac{Cd\mu_y}{2a}\right), \tag{22}$$

$$F_z = -\frac{1}{2}\rho C_l bc\Omega^2 R^3\left(\frac{1}{2}\lambda + \left(\frac{1}{2}{\mu_x}^2 + \frac{1}{3} + \frac{1}{2}{\mu_y}^2\right)\theta_{\text{col}} + \frac{1}{4}\left(1 + {\mu_x}^2 + {\mu_y}^2\right)\theta_t + \frac{1}{2}\left(\theta_{\text{lat}}\mu_y - \theta_{\text{lon}}\mu_x\right)\right). \tag{23}$$

C. Induced Inflow

Momentum theory assumes that the rotor behaves like a circular wing and thrust ($T = -F_z$) is generated when the rotor moves air downwards through what is assumed to be a virtual tube. The amount of thrust generated is determined by the change of momentum for the air when it is moved by the rotor from far above the helicopter (upstream) to far below the helicopter (downstream). As the steam tube is assumed a closed system, the mass flux is constant through it and therefore the change of momentum is generated by

the air velocity change. This velocity change comes from the induced velocity v_i and relates to the thrust as

$$T = 2\rho A|v|v_i \Leftrightarrow v_i = \frac{T}{2\rho A\sqrt{{w_x}^2 + {w_y}^2 + (w_z - v_i)^2}}.$$

A dimensionless thrust coefficient C_T is in introduced

$$C_T = \frac{T}{\rho A(\Omega R)^2}, \tag{24}$$

and substituted together with the expression for v_i into the inflow ratio λ

$$\lambda = \frac{w_z - v_i}{\Omega R} = \mu_z - \frac{C_T}{2\sqrt{(\mu_x^2 + \mu_y^2) + \lambda^2}}, \tag{25}$$

and λ is then found by analytically solving this fourth order equation.

III. FEEDFORWARD CONTROL

Feedforward control is used to compensate for measured disturbances before they affect the system output. Ideally, given a perfect model of the system and an error free measurement of the disturbance, it is possible to entirely eliminate the effect of the disturbance. However, in reality with modeling approximations and measurement noise, feedforward control is seen as a tool to be used together with feedback control and thereby improve performance over systems with only feedback control.

In the helicopter case, a feedforward controller could be designed to counter wind disturbance if it is possible to invert the model such that the control signals can be calculated from the disturbance and helicopter states. Furthermore, it is necessary to use the feedforward in combination with a feedback controller that can stabilize the helicopter and do trajectory tracking. The full control architecture is shown in figure 2. A wind gust on a helicopter will cause a upward

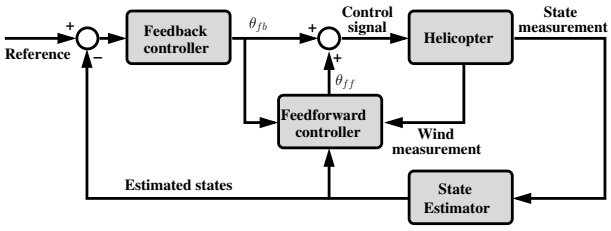

Fig. 2. Combined feedback and feedforward control.

motion and a motion along with the wind where the upward motion is normally the stronger and the sideways motion the weaker effect. This means that both collective and cyclic control signals are needed to counter the disturbance.

The design of the feedforward controller includes a inversion of the helicopter model such that control signals can be calculated given wind and helicopter states. A step-wise approach is taken as an inversion of the full helicopter model mathematically cumbersome. A decoupling between the different axis is assumed such that the collective pitch couples mainly to the thrust and that the lateral and longitudinal pitch couples to the lateral and longitudinal force, respectively. Control of the tail will be neglected in this feedforward controller as the gyro system that controls the tail on most small scale helicopters has a very good disturbance rejection. However, the tail-yaw model equations could easily be included in the approach. Furthermore, it is observed that while changes in collective pitch have significant influence on the lateral and longitudinal forces, changes in cyclic pitch have little influence on the thrust. Therefore, the feedforward controller is synthesized by first calculating the collective pitch given the disturbance in x,y and z. This is then using that in the calculation of the lateral and longitudinal cyclic pitch.

The main idea behind the controller is to use the helicopter model to calculate the no-disturbance force, i.e. the force that would have resulted if there was no disturbance. This desired force, which can be considered as a reference for the controller, is then used in the inverted model with the disturbance present and the resulting control signal will result in the correct force for the given disturbance.

To calculate the no-disturbance model response (1) is calculated without wind disturbance as

$$\mu_x^* = \frac{v_x}{\Omega R},\ \mu_y^* = \frac{v_y}{\Omega R},\ \mu_z^* = \frac{v_z}{\Omega R},\ \lambda^* = \frac{v_z - v_i}{\Omega R}, \tag{26}$$

where * indicates no-disturbance variable. The first step is to calculate the no-disturbance inflow ratio using the analytical solution to (25) as

$$\lambda^* = f_{(25)}(\mu^*, \theta_{\text{col,fb}}, \theta_{\text{lat,fb}}, \theta_{\text{lon,fb}}), \tag{27}$$

which is then used in the calculation of the no-disturbance thrust

$$F_z^* = f_{(23)}(\lambda^*, \mu^*, \theta_{\text{col,fb}}, \theta_{\text{lat,fb}}, \theta_{\text{lon,fb}}). \tag{28}$$

where $f_{(23)}$ is equation 23 as a function. We can then find the collective pitch that will result in a thrust force F_z^* given the disturbance. The corresponding λ given the disturbance is calculated

$$\lambda_{\text{ff}} = f_{(25)}(\mu, F_z^*), \tag{29}$$

and used in the final calculation of the feedforward collective pitch which is found trivially as (23) solved for θ_{col}

$$\theta_{\text{col,ff}} = f_{(23)}^{-1}(\mu, F_z^*, \theta_{\text{lat,fb}}, \theta_{\text{lon,fb}}), \tag{30}$$

where $f_{(23)}^{-1}$ represent the model inversion of (23).

The procedure for the lateral and longitudinal axis is similar to the vertical axis. First the no-disturbance forces are calculated

$$a_{\text{lat}}^* = f_{(15)}(\mu^*, \lambda_{\text{ff}}, \theta_{\text{col,ff}}, \theta_{\text{lat,fb}}), \tag{31}$$
$$a_{\text{lon}}^* = f_{(16)}(\mu^*, \lambda_{\text{ff}}, \theta_{\text{col,ff}}, \theta_{\text{lon,fb}}), \tag{32}$$
$$F_y{}^* = f_{(22)}(\mu^*, \lambda_{\text{ff}}, a_{\text{lat}}^*, \theta_{\text{lat,ff}}), \tag{33}$$
$$F_x{}^* = f_{(21)}(\mu^*, \lambda_{\text{ff}}, a_{\text{lon}}^*, \theta_{\text{lon,ff}}). \tag{34}$$

For the next step, the flapping equations (15) and (16) are substituted into (21) and (22). The resulting (second order)

equations are then solved for θ_{lat} and θ_{lon}, respectively

$$\theta_{\text{lat,ff}} = f^{-1}_{(15),(22)}(\mu, \lambda_{\text{ff}}, \theta_{\text{col,ff}}), \tag{35}$$

$$\theta_{\text{lon,ff}} = f^{-1}_{(16),(21)}(\mu, \lambda_{\text{ff}}, \theta_{\text{col,ff}}). \tag{36}$$

The final feedforward controller output is calculated as

$$\theta_{\text{ff}} = \begin{bmatrix} \theta_{\text{col,ff}} \\ \theta_{\text{lat,ff}} \\ \theta_{\text{lon,ff}} \end{bmatrix} - \begin{bmatrix} \theta_{\text{col,fb}} \\ \theta_{\text{lat,fb}} \\ \theta_{\text{lon,fb}} \end{bmatrix}, \tag{37}$$

were the subtraction of θ_{fb} is done to ensure that the feedforward controller generates perturbations from the feedback control trajectory. If no disturbance is present, the feedforward equations simply calculates back and forth and result in $\theta_{\text{col,fb}} = \theta_{\text{col,ff}}$ etc. which then in turn result in a zero θ_{ff}.

If the helicopter used is a fixed pitch type, which means that the thrust is controlled through main rotor speed Ω, it can be accommodated by solving (23) for Ω, considering θ_{col} as a constant, and using the result instead of (30)

$$\Omega_{\text{ff}} = f_{(23)}(\mu, F_z^*, \theta_{\text{lat,fb}}, \theta_{\text{lon,fb}}). \tag{38}$$

IV. DISTURBANCE MEASUREMENT

In order to counter the disturbance on helicopter it is necessary to have a measurement or estimate of it. The disturbance in this case is wind which is difficult to predict and a wind measurement is therefore necessary. When measuring the wind at the helicopter, a number of challenges arise. The most obvious one is that the helicopter itself generates air flow, both from motion and from the rotors. The motion of the helicopter is known from the state estimator and the body velocities can be extracted from the wind measurements. The induced velocity from the rotor is more difficult to isolate and remove, but can be predicted using (25), and then subtracted. With the helicopter induced air flow subtracted, a measurement of the external wind is available. More theoretical and practical focus will be put on this in a near future publication.

V. RESULTS

The control scheme will here be illustrated used on a small scale autonomous helicopter: The Aalborg University Corona Rapid Prototyping Platform which is a 1 kg fixed pitch electric helicopter. It performs fully autonomous flight with landings and takeoff using a set of gain-scheduled PID controllers. There is no computer onboard the helicopter and all control and estimation computation is done on ground in real time. It is powered from a power supply on the ground through wires that hangs from the nose of the helicopter and control signals to the servos are transmitted through a standard RC system. Helicopter state measurements are acquired using a Vicon motion tracking system at 100 Hz and with a sufficient accuracy for these to be considered as true values.

The laboratory is equipped with three Big Bear II fans with a diameter of 0.6 m, each capable of delivering wind of up to 16 m/s at 1 m distance. With these it is possible to deliver a controllable and known wind disturbance to the helicopter.

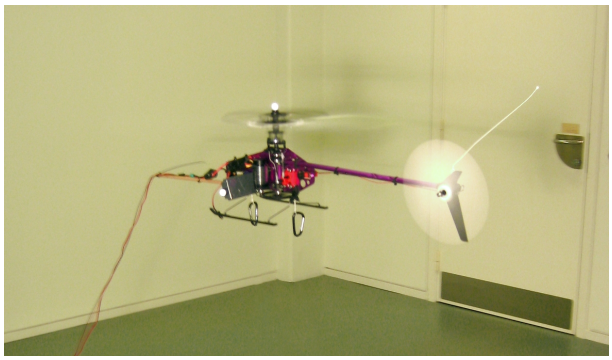

Fig. 3. The Aalborg University Corona Rapid Prototyping Platform.

Two different flight tests have been carried out: In the first, the helicopter hovers in front of the fans which are then turned on, which is equivalent to a wind gust. In the second the helicopter flies through the wind stream of the running fans which is equivalent to the helicopter flying through cross winds in a road intersection.

The wind sensor used in these tests is a R.M. Young 81000 3D ultrasonic anemometer (32 Hz measurement with 1% accuracy). However, this sensor is both too big and too heavy to be mounted on the small helicopter and therefore different approaches are taken in the two tests to provide the feedforward controller with wind measurements without the sensor being mounted on the helicopter.

A. Flight Test: Gust disturbance

In the gust disturbance test, two fans are use. The fans are separate by some distance and does not influence each other. Two meters in front of the one fan the helicopter hovers with the nose pointing towards the fan. At the same distance, but in front of the other fan the wind sensor is placed. The two fans are controlled together and this means that the sensor will (ideally) see the same wind as the helicopter. A gust is emulated by turning the fans on and off in rapid succession and the helicopter response with and without feedforward is observed. The response of the helicopter to the gusts is shown in figure 4 and the actual wind gusts are shown in figure 5.

It can be seen how the gust results in first an upward and backward motion and as the wind subsides a downward and forward motion. It is also evident how the use of the feedforward controller significantly reduces the deviations of helicopter due to the gust compared to the response without the feedforward controller.

B. Flight Test: Cross wind disturbance

In the cross wind disturbance test the helicopter flies sideways past the fan and thereby crossing in and out of the wind stream. The wind velocity estimation is done by measuring wind velocity as a function of position in front of the fan (using the anemometer) prior to flight and the during

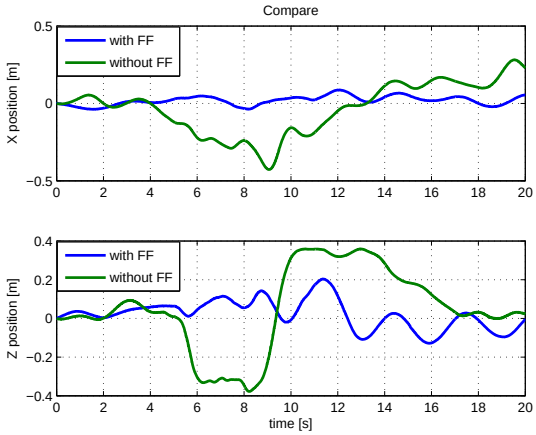

Fig. 4. Helicopter gust response with and without feedforward.

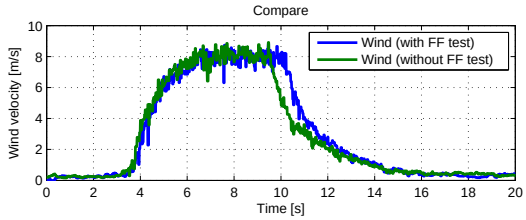

Fig. 5. Wind gusts recorded in the test of helicopter response with and without feedforward.

flight use interpolation on these measurements to predict the wind that the helicopter encounters at varying positions.

The response of the helicopter flying though the wind is shown in figure 6 and as before it can be seen how the feedforward is capable of reducing the helicopter response to the wind. The response can also be seen on figure 7 where

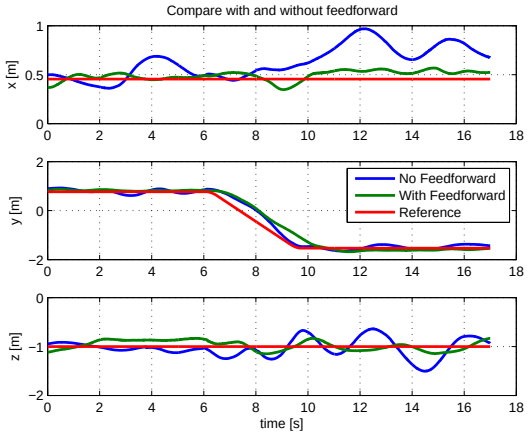

Fig. 6. Helicopter cross wind response with and without feedforward.

the location of the wind corridor is also indicated.

VI. DISCUSSIONS AND FUTURE WORKS

A. Discussion

It has been demonstrated how a feedforward controller can be used, in augmentation with a feedback controller, to

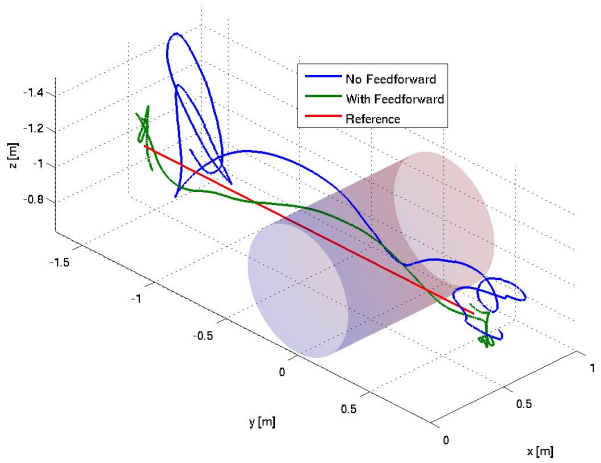

Fig. 7. 3D plot of helicopter cross wind response with and without feedforward.

counter disturbances from external wind. The approach, that involves calculating feedforward control signals to cancel the additional force from the wind, has been demonstrated to improve tracking performance in real flight. Even though the control scheme is based on model inversion, due to the reduced computation complexity that arises from the simplified model, the proposed method poses no problem for real time implementation. As the method is based on a feedforward approach, it is important that the model has a good correspondence with the actual behavior of the system to ensure an acceptable performance.

B. Future Works

Results on the theory and practice behind reliable wind measurements on a helicopter will be published in a near future. This includes detailed considerations on sensor types, more advanced helicopter inflow modeling, as well as measurement experiments. Furthermore, outdoor flight tests are to be carried out in uncontrolled wind settings.

REFERENCES

[1] E. Wan, A. Bogdanov, R. Kieburtz, A. Baptista, M. Carlsson, Y. Zhang, and M. Zulauf, *Software Enabled Control: Information Technologies for Dynamical Systems*. John Wiley & Sons, 2003, ch. 10, Model predictive neural control for aggressive helicopter maneuvers.

[2] A. Bogdanov, E. Wan, and G. Harvey, "Sdre flight control for x-cell and r-max autonomous helicopters," in *The 43rd IEEE Conference on Decision and Control*, 2004.

[3] E. N. Johnson and S. K. Kannan, "Adaptive trajectory control for autonomous helicopters," *AIAA Journal of Guidance, Control, and Dynamics, Vol 28, No 3*, 2005.

[4] K. A. Danapalasingam, A. la Cour-Harbo, and M. Bisgaard, "Feedforward control of an autonomous helicopter using trim inputs," in *AIAA Infotech@Aerospace & AIAA Unmanned...Unlimited Conference and Exhibit*, 2009.

[5] ——, "Disturbance effects in nonlinear control systems and feedforward control strategy," in *7th International Conference on Control and Automation*, 2009.

[6] E. van der Hooft and T. van Engelen, "Estimated wind speed feed forward control for wind turbine operation optimisation," in *European wind energy conference*, 2004.

[7] M. Bisgaard, "Modeling, estimation, and control of helicopter slung load system," Ph.D. dissertation, Aalborg University, 2008.